Mitigation of Alfvén Eigenmodes in Negative Triangularity plasmas at TCV

P. Oyola, M. García-Muñoz, M. Vallar, E. Viezzer, J. Rueda-Rueda, J. Domínguez-Palacios, J. Gonzalez-Martin, Y. Todo, S. Sharapov, A. Fasoli, B. Duval, A. Karpushov, S. Coda, O. Sauter and the TCV team.

PSFT Plasma Science and Fusion Technology
Universidad de Sevilla
EPFL

This work has been carried out within the framework of the EUROfusion Consortium and has received funding from the Euratom research and training programme 2014-2018 and 2019-2020 under grant agreement No 633053. The views and opinions expressed herein do not necessarily reflect those of the European Commission.

Outline

- Experimental observations of TAEs in NT
- MEGA: 3D nonlinear hybrid kinetic-MHD
- TAEs in NT and PT
- Wave-particle resonances in the FI phase-space
- Fast-ion losses induced by TAE in NT and PT

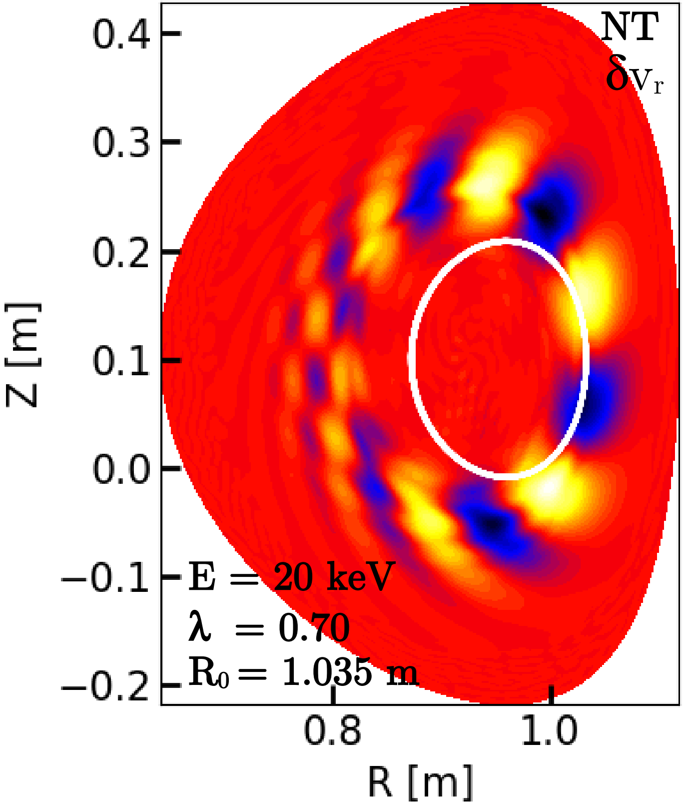

- Experimental observations of TAEs in NT
- MEGA: 3D nonlinear hybrid kinetic-MHD
- TAEs in NT and PT
- Wave-particle resonances in the FI phase-space
- Fast-ion losses induced by TAE in NT and PT

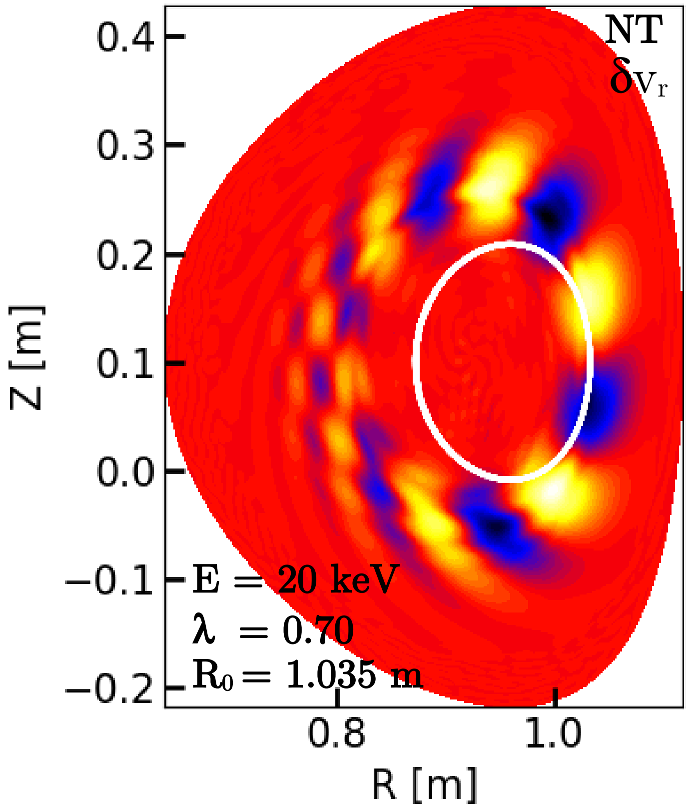

AEs in NT firstly observed in DIII-D

- Experiments in DIII-D[4] to obtain AEs, shows TAEs excited in NT and PT.

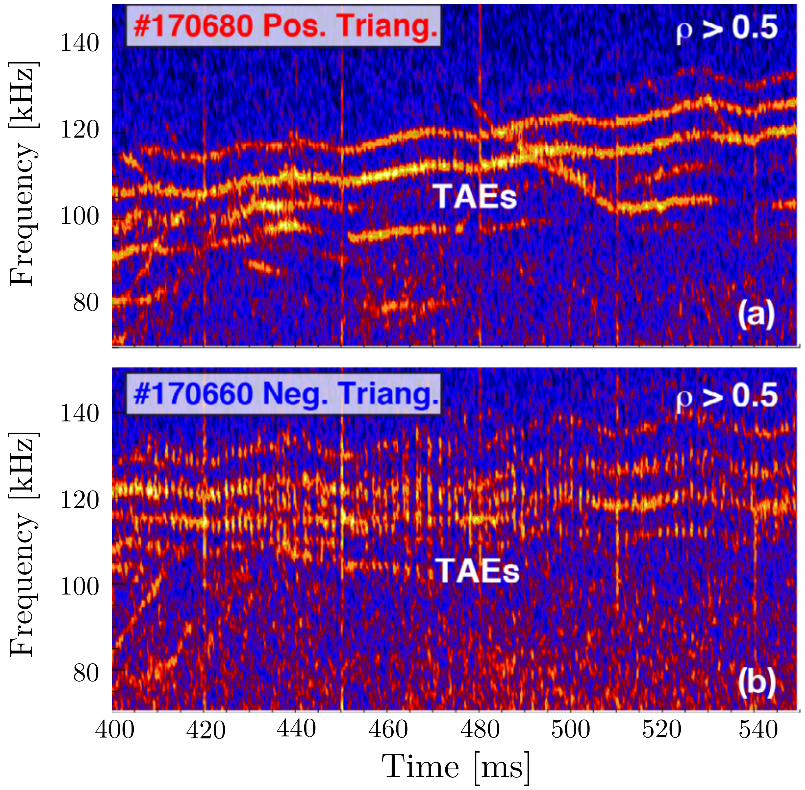

[4] M. A. Van Zeeland *et al.*, NF **59** 086028 (2019)

Gyrofluid simulations indicate negligible impact on AE activity

- Experiments in DIII-D[4] to obtain AEs, shows TAEs excited in NT and PT.

- Numerical studies[5] with FAR3d[6]:
  - Linear EP-driven AE.
  - 2-moments gyrofluid model for FI
  - Negligible impact of triangularity on AE growth rate

$\phi_{ES}^{n=3}(R,z)$

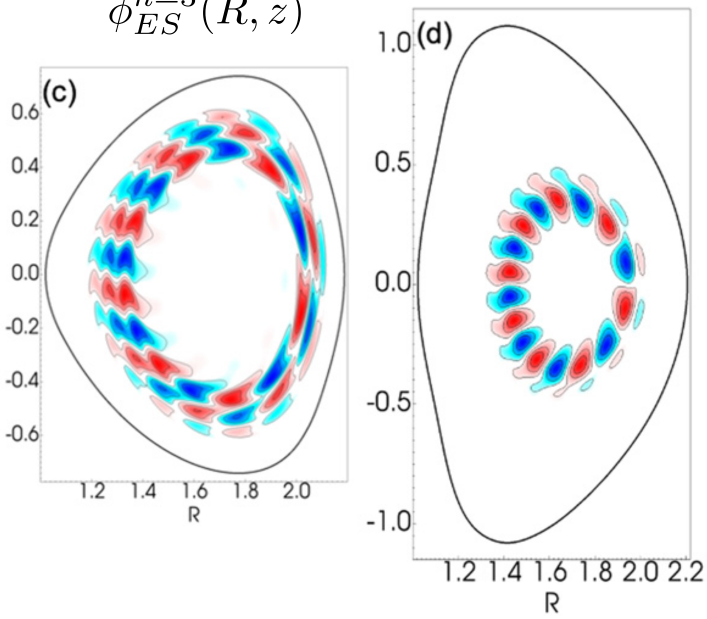

[4] M. A. Van Zeeland *et al.*, NF **59** 086028 (2019)
[5] Y. Ghai *et al.*, NF **61** 126020 (2021)
[6] L. A. Charlton *et al.*, J. Comp. Phys **86** 270 (1990)

Strong NT impact on AEs at TCV

- Strong impact of triangularity on Alfvénic modes:
  - Amplitude reduction
  - Frequency drops

- Uncontrolled changes in many variables:
  - Density rise during NT phase (better confinement)
  - Direct comparison between triangularities is difficult.

- Nonlinear hybrid simulations help unreveal the impact of δ in the Alfvén Eigenmodes and induced fast-ion transport.

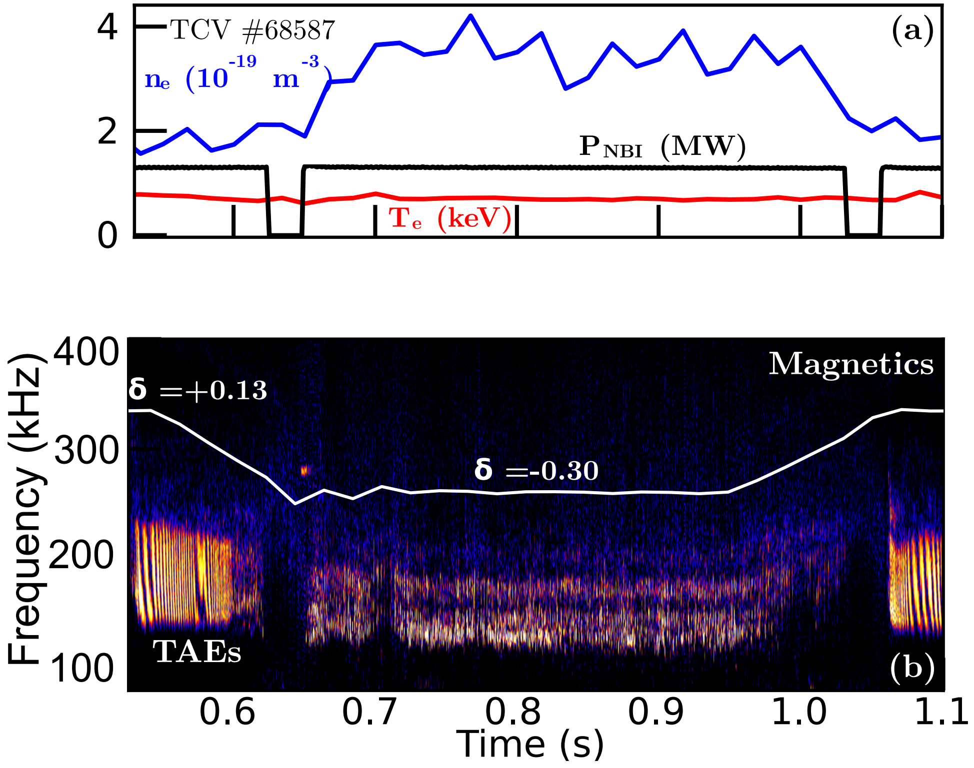

- Experimental observations of TAEs in NT
- MEGA: 3D nonlinear hybrid kinetic-MHD
- TAEs in NT and PT
- Wave-particle resonances in the FI phase-space
- Fast-ion losses induced by TAE in NT and PT

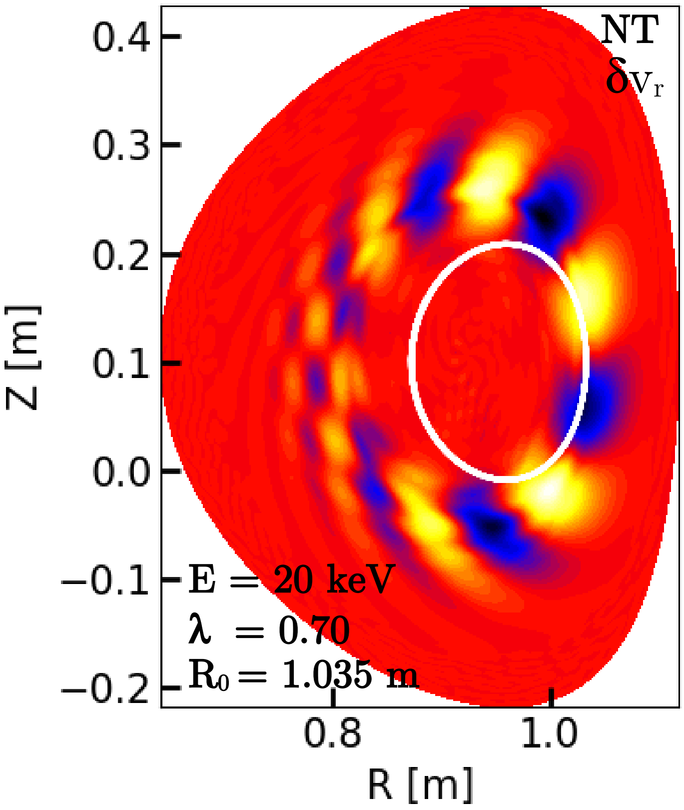

MEGA[7]: Nonlinear 3D hybrid kinetic-MHD code

Bulk plasma

- Full resistive-MHD model.

$$\frac{\partial \rho}{\partial t} + \vec{\nabla} \cdot (\rho \vec{v}) = \vec{\nabla} \cdot \left(\nu_n \vec{\nabla} \rho \right)$$

$$\frac{\partial \vec{U}}{\partial t} + \left(\vec{v} \cdot \vec{\nabla} \right) \vec{U} = -\vec{\nabla} p + \left(\vec{J} - \vec{J}_{FI} \right) \times \vec{B}$$
$$+ \frac{4}{3} \left(\nu \rho \vec{\nabla} \cdot \vec{v} \right) - \vec{\nabla} \times (\nu \rho \vec{\omega})$$

$$\frac{\partial p}{\partial t} + \vec{\nabla} \cdot (p \vec{v}) + (\gamma - 1)\, p \vec{\nabla} \cdot \vec{v} =$$
$$\vec{\nabla} \cdot \left(\chi \vec{\nabla} \left(p - p_{eq} \right) \right)$$
$$(\gamma - 1) \left[\nu \rho \left(\vec{\nabla} \times \vec{v} \right)^2 + \frac{4}{3} \left(\vec{\nabla} \cdot \vec{v} \right)^2 \right]$$
$$(\gamma - 1)\, \eta \left(\vec{J} - \vec{J}_{FI} \right) \cdot \left(\vec{J} - \vec{J}_{eq} \right)$$

$$\vec{E} = -\vec{v} \times B + \eta \vec{J}$$

[7] Y. Todo *et al.*, PoP **5** 1321 (1998)

MEGA[7]: Nonlinear 3D hybrid kinetic-MHD code

Bulk plasma

- Full resistive-MHD model.

$$\frac{\partial \rho}{\partial t} + \vec{\nabla} \cdot (\rho \vec{v}) = \vec{\nabla} \cdot \left(\nu_n \vec{\nabla} \rho \right)$$

$$\frac{\partial \vec{U}}{\partial t} + \left(\vec{v} \cdot \vec{\nabla} \right) \vec{U} = -\vec{\nabla} p + \left(\vec{J} - \vec{J}_{FI} \right) \times \vec{B}$$
$$+ \frac{4}{3} \left(\nu \rho \vec{\nabla} \cdot \vec{v} \right) - \vec{\nabla} \times (\nu \rho \vec{\omega})$$

Fast-ions

- *Kinetic description*: markers sampling distribution function.
- Gyrokinetic equation (δf or *full*-f).

$$\frac{\partial p}{\partial t} + \vec{\nabla} \cdot (p \vec{v}) + (\gamma - 1)\, p \vec{\nabla} \cdot \vec{v} =$$
$$\vec{\nabla} \cdot \left(\chi \vec{\nabla} (p - p_{eq}) \right)$$
$$(\gamma - 1) \left[\nu \rho \left(\vec{\nabla} \times \vec{v} \right)^2 + \frac{4}{3} \left(\vec{\nabla} \cdot \vec{v} \right)^2 \right]$$
$$(\gamma - 1)\, \eta \left(\vec{J} - \vec{J}_{FI} \right) \cdot \left(\vec{J} - \vec{J}_{eq} \right)$$

$$\vec{E} = -\vec{v} \times B + \eta \vec{J}$$

[7] Y. Todo *et al.*, PoP **5** 1321 (1998)

MEGA[7]: Nonlinear 3D hybrid kinetic-MHD code

Bulk plasma

- Full resistive-MHD model.

⬍ **Coupling through current density**

Fast-ions

- *Kinetic description*: markers sampling distribution function.
- Gyrokinetic equation (δf or *full*-f).

$$\frac{\partial \rho}{\partial t} + \vec{\nabla}\cdot(\rho\vec{v}) = \vec{\nabla}\cdot\left(\nu_n \vec{\nabla}\rho\right)$$

$$\frac{\partial \vec{U}}{\partial t} + \left(\vec{v}\cdot\vec{\nabla}\right)\vec{U} = -\vec{\nabla}p + \left(\vec{J} - \vec{J}_{FI}\right)\times\vec{B} + \frac{4}{3}\left(\nu\rho\vec{\nabla}\cdot\vec{v}\right) - \vec{\nabla}\times(\nu\rho\vec{\omega})$$

$$\frac{\partial p}{\partial t} + \vec{\nabla}\cdot(p\vec{v}) + (\gamma-1)\,p\vec{\nabla}\cdot\vec{v} = \vec{\nabla}\cdot\left(\chi\vec{\nabla}\left(p - p_{eq}\right)\right) (\gamma-1)\left[\nu\rho\left(\vec{\nabla}\times\vec{v}\right)^2 + \frac{4}{3}\left(\vec{\nabla}\cdot\vec{v}\right)^2\right] (\gamma-1)\,\eta\left(\vec{J}-\vec{J}_{FI}\right)\cdot\left(\vec{J}-\vec{J}_{eq}\right)$$

$$\vec{E} = -\vec{v}\times B + \eta\vec{J}$$

[7] Y. Todo *et al.*, PoP **5** 1321 (1998)

MEGA[7]: Nonlinear 3D hybrid kinetic-MHD code

Bulk plasma

- Full resistive-MHD model.

Coupling through current density

Fast-ions

- *Kinetic description*: markers sampling distribution function.
- Gyrokinetic equation (δf or *full*-f).

- 4th order finite differences in **cylindrical** coordinates (R, ϕ, z).

$$\frac{\partial \rho}{\partial t} + \vec{\nabla}\cdot(\rho\vec{v}) = \vec{\nabla}\cdot\left(\nu_n \vec{\nabla}\rho\right)$$

$$\frac{\partial \vec{U}}{\partial t} + \left(\vec{v}\cdot\vec{\nabla}\right)\vec{U} = -\vec{\nabla}p + \left(\vec{J} - \vec{J}_{FI}\right)\times\vec{B} + \frac{4}{3}\left(\nu\rho\vec{\nabla}\cdot\vec{v}\right) - \vec{\nabla}\times\left(\nu\rho\vec{\omega}\right)$$

$$\frac{\partial p}{\partial t} + \vec{\nabla}\cdot(p\vec{v}) + (\gamma-1)\,p\vec{\nabla}\cdot\vec{v} =$$

$$\vec{\nabla}\cdot\left(\chi\vec{\nabla}\left(p - p_{eq}\right)\right)$$

$$(\gamma-1)\left[\nu\rho\left(\vec{\nabla}\times\vec{v}\right)^2 + \frac{4}{3}\left(\vec{\nabla}\cdot\vec{v}\right)^2\right]$$

$$(\gamma-1)\,\eta\left(\vec{J} - \vec{J}_{FI}\right)\cdot\left(\vec{J} - \vec{J}_{eq}\right)$$

$$\vec{E} = -\vec{v}\times B + \eta\vec{J}$$

[7] Y. Todo *et al.*, PoP **5** 1321 (1998)

MEGA[7]: Nonlinear 3D hybrid kinetic-MHD code

PSFT Plasma Science and Fusion Technology EPFL

Bulk plasma

- Full resistive-MHD model.

Coupling through current density

Fast-ions

- *Kinetic description*: markers sampling distribution function.
- Gyrokinetic equation (δf or *full*-f).

- 4th order finite differences in **cylindrical** coordinates (R, ϕ, z).
- Explicit 4th Runge-Kutta for time-integration.

$$\frac{\partial \rho}{\partial t} + \vec{\nabla}\cdot(\rho\vec{v}) = \vec{\nabla}\cdot\left(\nu_n\vec{\nabla}\rho\right)$$

$$\frac{\partial \vec{U}}{\partial t} + \left(\vec{v}\cdot\vec{\nabla}\right)\vec{U} = -\vec{\nabla}p + \left(\vec{J} - \vec{J}_{FI}\right)\times\vec{B} + \frac{4}{3}\left(\nu\rho\vec{\nabla}\cdot\vec{v}\right) - \vec{\nabla}\times(\nu\rho\vec{\omega})$$

$$\frac{\partial p}{\partial t} + \vec{\nabla}\cdot(p\vec{v}) + (\gamma-1)\,p\vec{\nabla}\cdot\vec{v} = \vec{\nabla}\cdot\left(\chi\vec{\nabla}\left(p - p_{eq}\right)\right)$$
$$(\gamma-1)\left[\nu\rho\left(\vec{\nabla}\times\vec{v}\right)^2 + \frac{4}{3}\left(\vec{\nabla}\cdot\vec{v}\right)^2\right]$$
$$(\gamma-1)\,\eta\left(\vec{J} - \vec{J}_{FI}\right)\cdot\left(\vec{J} - \vec{J}_{eq}\right)$$

$$\vec{E} = -\vec{v}\times B + \eta\vec{J}$$

[7] Y. Todo *et al.*, PoP **5** 1321 (1998)

Simulation setup for the δ comparison

- Flipped equilibrium to isolate the +δ / -δ effects on AE activity[8].

Simulation parameters

- δf-method for kinetic species.
- #markers = 23M particles
- Multi-*n* simulation (n < 5)

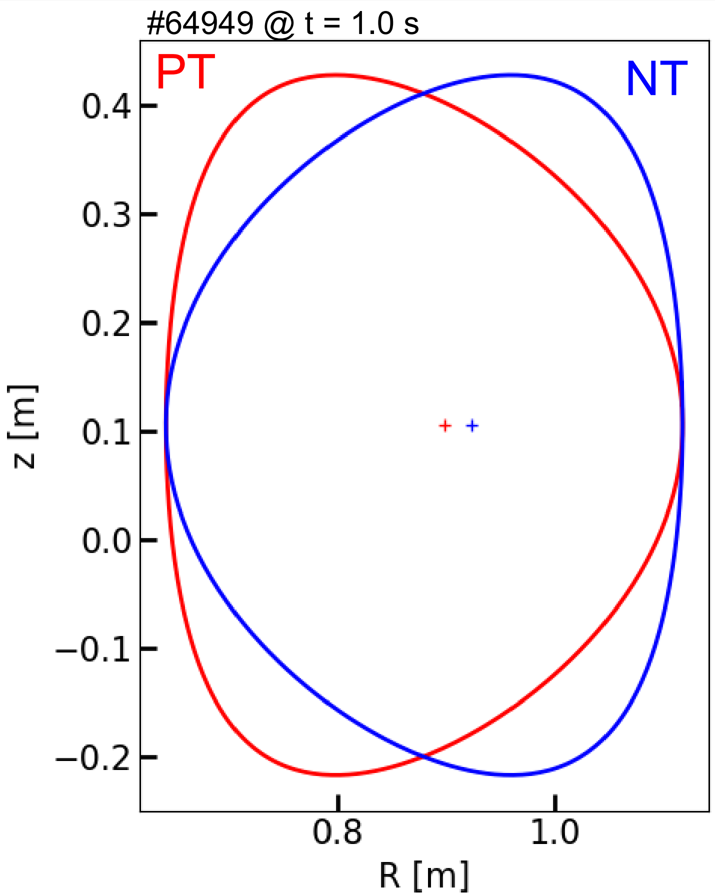

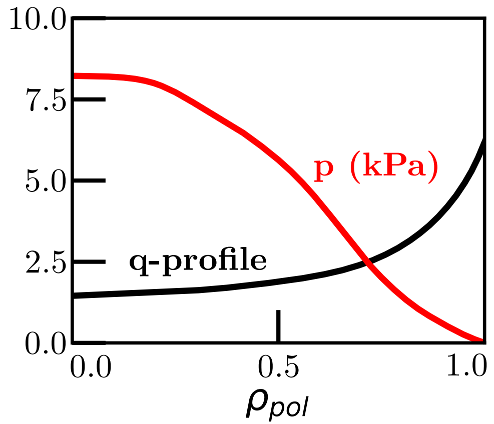

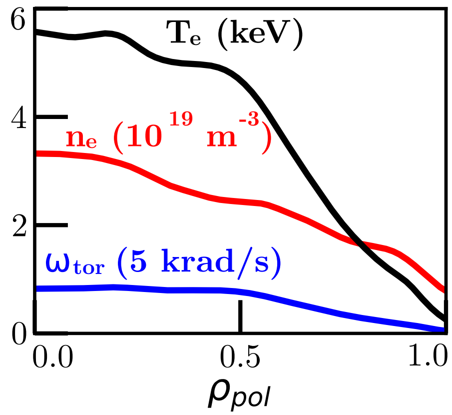

[8] P. Oyola *et al.*, in preparation

Ad-hoc initial FI distribution

Analytical anisotropic slowing-down distribution

$$f_0 \propto e^{-\frac{(\rho-\rho_0)^2}{2(\Delta\rho_0)^2}} \frac{1}{v^3 + v_{crit}^3} erfc\left(\frac{v - v_{birth}}{\Delta v}\right) e^{-\frac{(\Lambda-\Lambda_0)^2}{2(\Delta\Lambda)^2}}$$

Ad-hoc initial FI distribution

Analytical anisotropic slowing-down distribution

$$f_0 \propto e^{-\frac{(\rho-\rho_0)^2}{2(\Delta\rho_0)^2}} \frac{1}{v^3 + v_{crit}^3} erfc\left(\frac{v - v_{birth}}{\Delta v}\right) e^{-\frac{(\Lambda-\Lambda_0)^2}{2(\Delta\Lambda)^2}}$$

Ad-hoc initial FI distribution

Analytical anisotropic slowing-down distribution

$$f_0 \propto e^{-\frac{(\rho-\rho_0)^2}{2(\Delta\rho_0)^2}} \frac{1}{v^3 + v_{crit}^3} erfc\left(\frac{v - v_{birth}}{\Delta v}\right) e^{-\frac{(\Lambda-\Lambda_0)^2}{2(\Delta\Lambda)^2}}$$

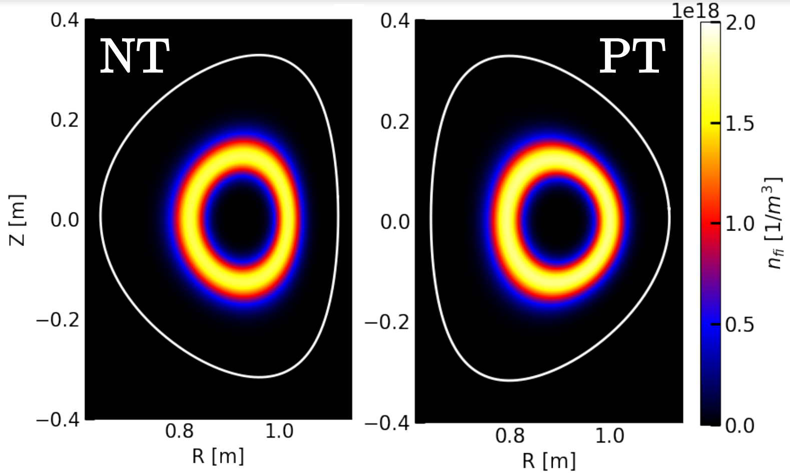

Ad-hoc initial FI distribution

Analytical anisotropic slowing-down distribution

$$f_0 \propto e^{-\frac{(\rho-\rho_0)^2}{2(\Delta\rho_0)^2}} \frac{1}{v^3 + v_{crit}^3} erfc\left(\frac{v - v_{birth}}{\Delta v}\right) e^{-\frac{(\Lambda-\Lambda_0)^2}{2(\Delta\Lambda)^2}}$$

$$\Lambda_0 \equiv \frac{\mu B_{\mathrm{axis}}}{E}$$

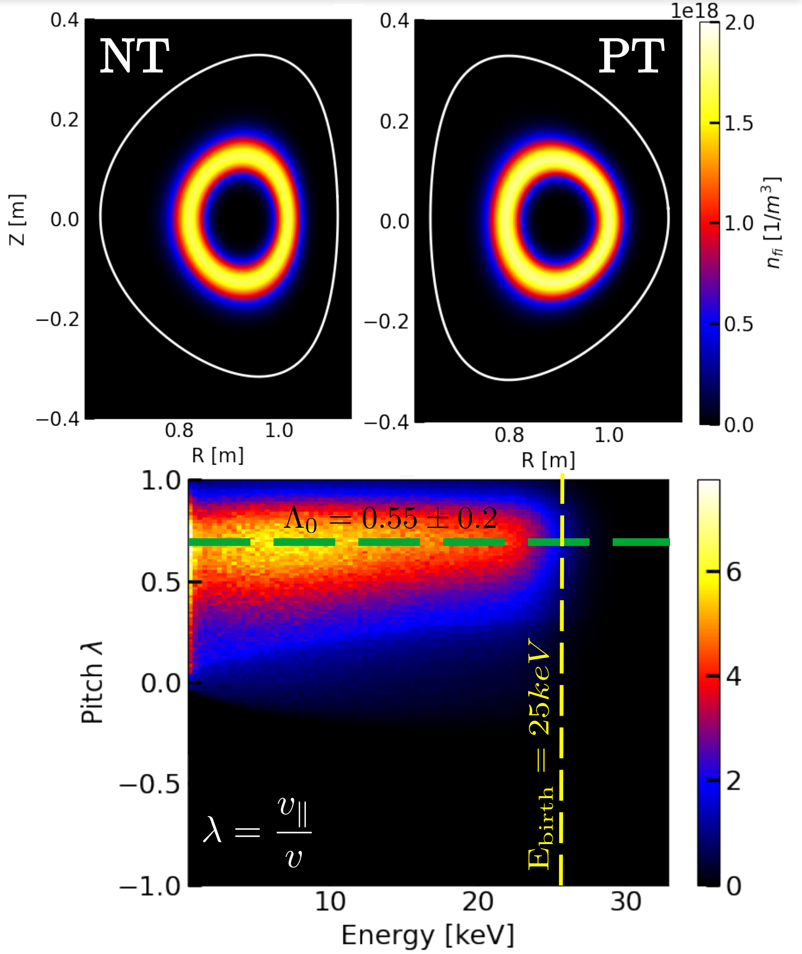

Ad-hoc initial FI distribution

Analytical anisotropic slowing-down distribution

$$f_0 \propto e^{-\frac{(\rho-\rho_0)^2}{2(\Delta\rho_0)^2}} \frac{1}{v^3 + v_{crit}^3} erfc\left(\frac{v - v_{birth}}{\Delta v}\right) e^{-\frac{(\Lambda-\Lambda_0)^2}{2(\Delta\Lambda)^2}}$$

- Scan in different pitch-angle injections $\Lambda_0 \equiv \frac{\mu B_{\text{axis}}}{E}$
- Scan in different fast-ion gradient location ρ_0

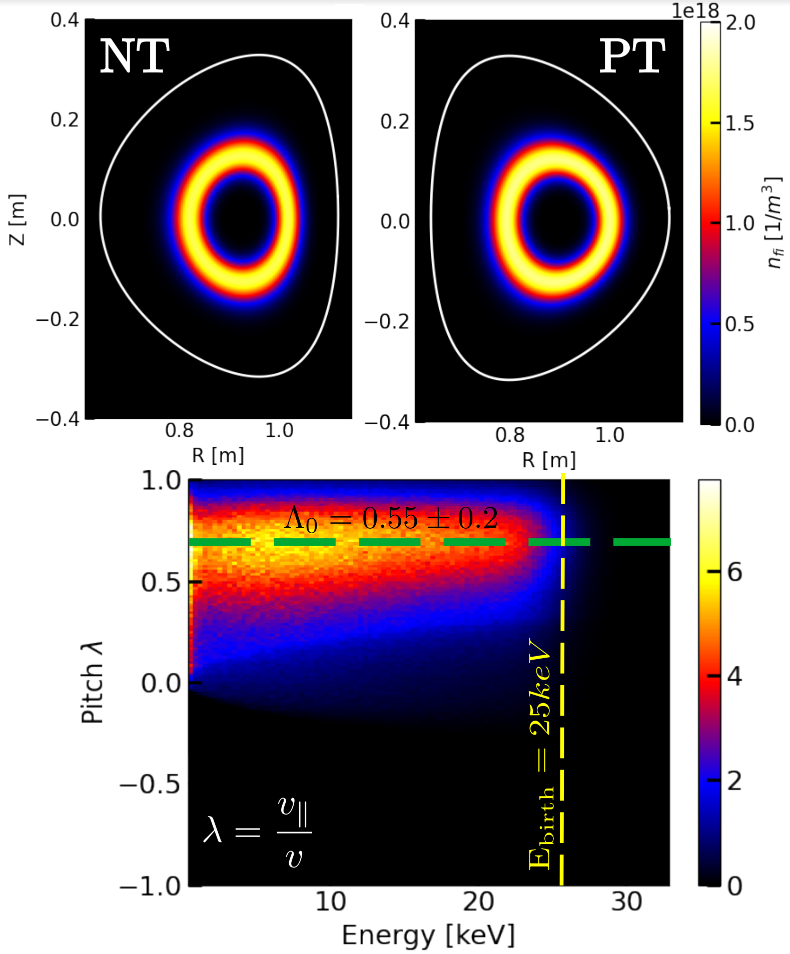

Initial FI drive is the same for NT and PT

Analytical slowing-down distribution:

$$f_0 \propto e^{-\frac{(\rho-\rho_0)^2}{2(\Delta\rho_0)^2}} \frac{1}{v^3 + v_{crit}^3} erfc\left(\frac{v - v_{birth}}{\Delta v}\right) e^{-\frac{(\Lambda-\Lambda_0)^2}{2(\Delta\Lambda)^2}}$$

- Scan in different pitch-angle injections $\Lambda_0 \equiv \frac{\mu B_{\text{axis}}}{E}$
- Scan in different fast-ion gradient location ρ_0

$$\gamma_{TAE} \propto \beta_{FI} \left(\frac{\partial f_0}{\partial E} + \frac{n}{\omega}\frac{\partial f_0}{\partial P_\phi}\right)$$

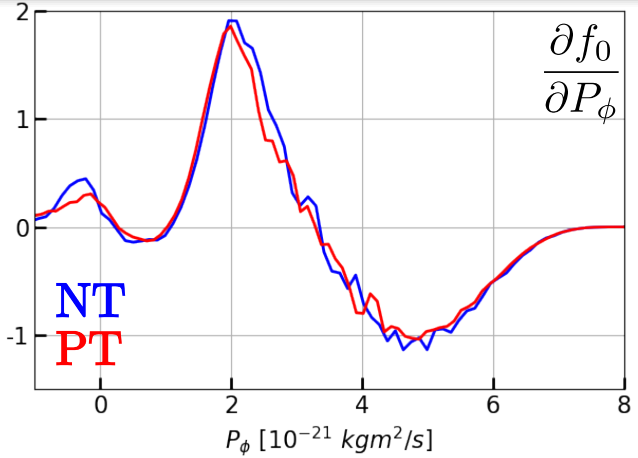

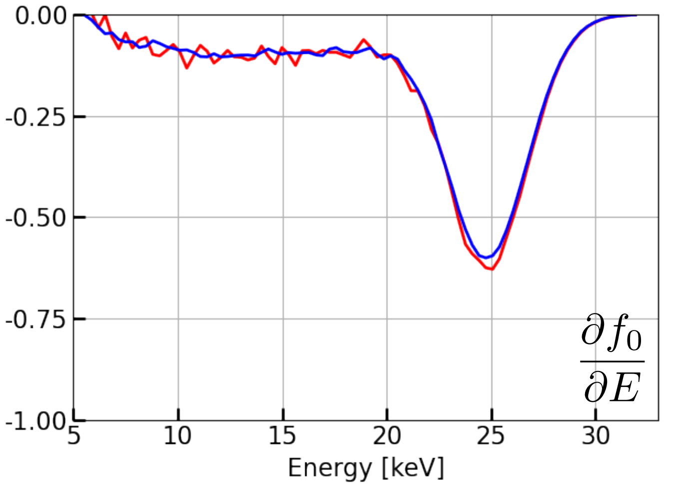

Outline

- Why Negative Triangularity ?
- MEGA: 3D nonlinear hybrid kinetic-MHD
- TAEs in NT and PT
- Wave-particle resonances in the FI phase-space
- Fast-ion losses induced by TAE in NT and PT

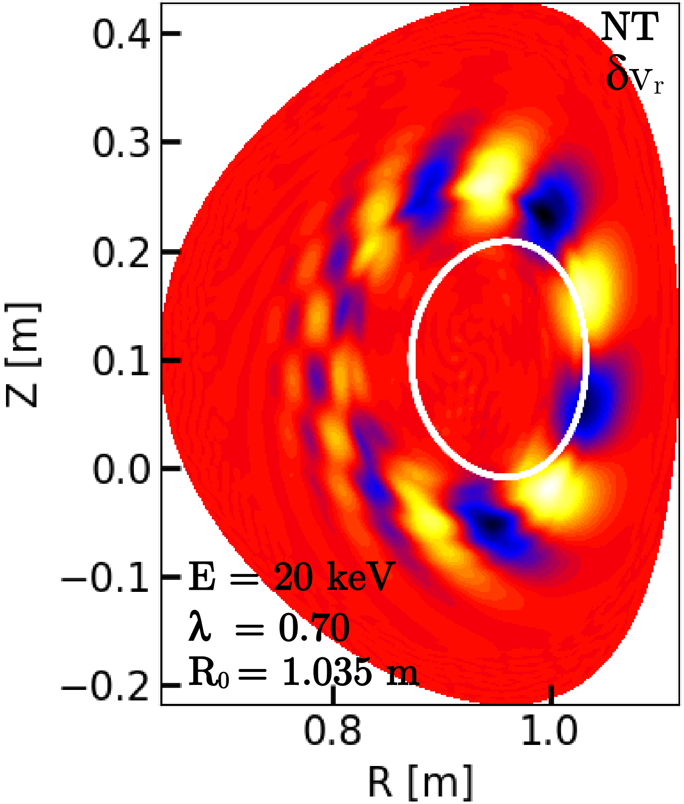

TAEs is mitigated in NT vs PT

TAEs appear both in PT and NT:

- PT reaches an energy ~40% higher.

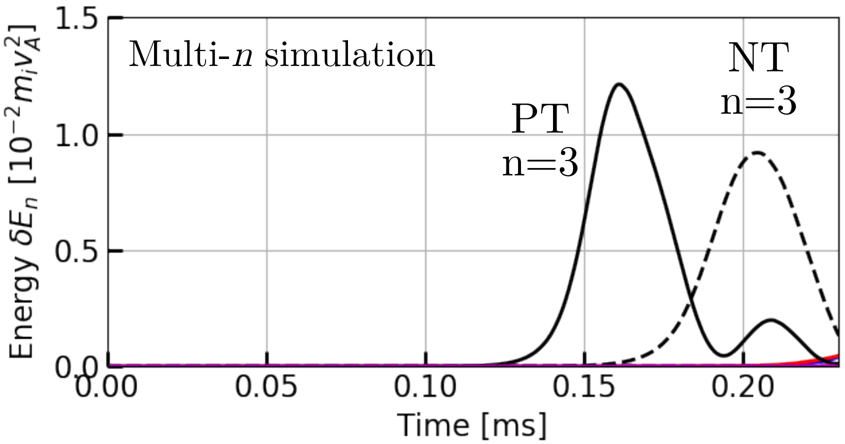

TAEs is mitigated in NT vs PT

TAEs appear both in PT and NT:

- PT reaches an energy ~40% higher.
- SAW is similar in PT & NT.

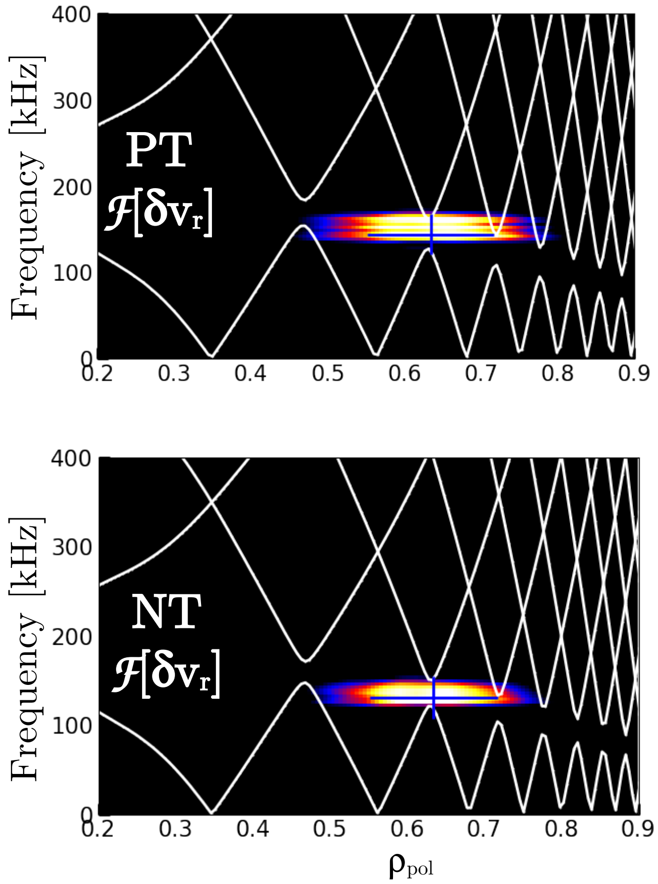

Linear growth rate for NT and PT

TAEs appear both in PT and NT:

- PT reaches an energy ~40% higher.
- SAW is similar in PT & NT.
- NT shows a smaller growth rate.

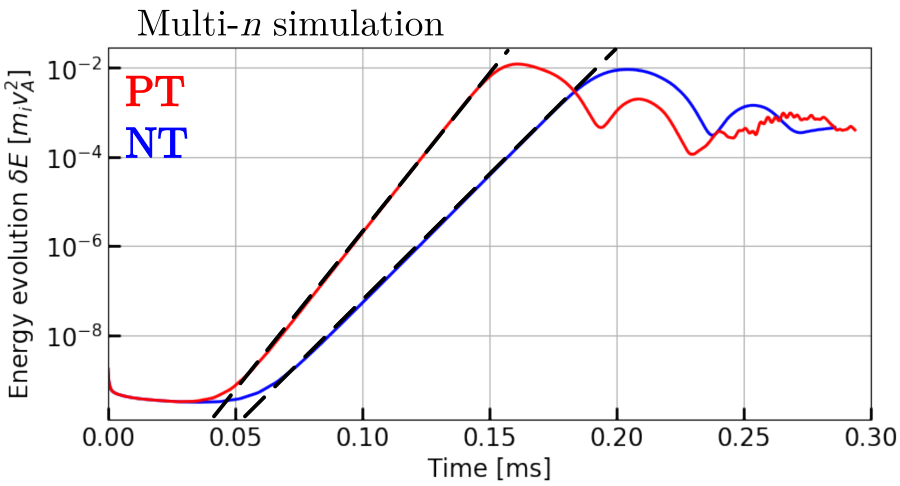

Linear growth rate for NT and PT

TAEs appear both in PT and NT:

- PT reaches an energy ~40% higher.
- SAW is similar in PT & NT.
- NT shows a smaller growth rate.
- This trend is kept independent on the pair of parameters Λ_0 and ρ_0.

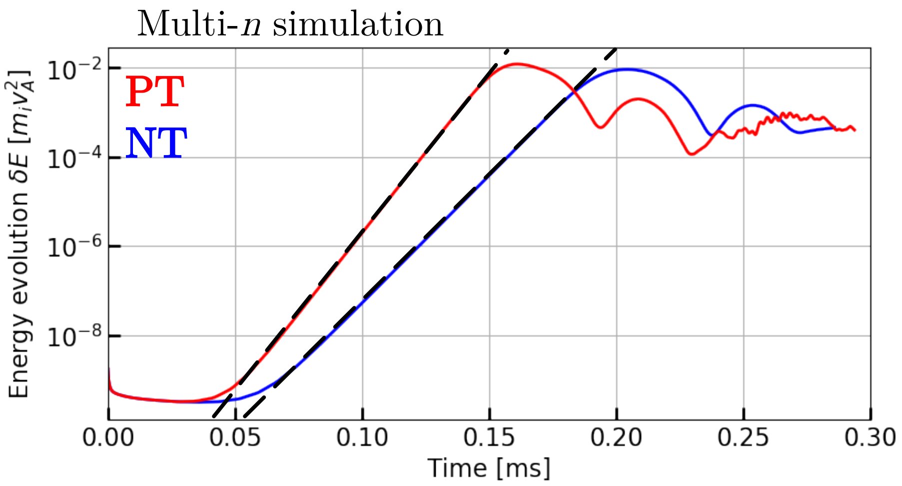

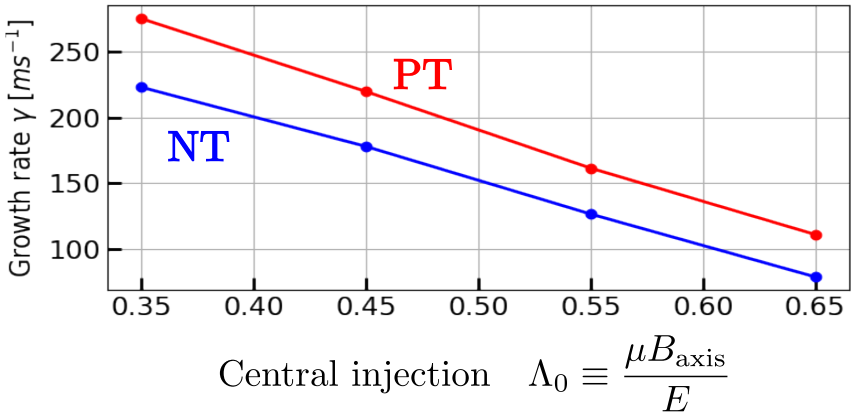

Linear growth rate for NT and PT

TAEs appear both in PT and NT:

- PT reaches an energy ~40% higher.
- SAW is similar in PT & NT.
- NT shows a smaller growth rate.
- This trend is kept independent on the pair of parameters Λ_0 and ρ_0.

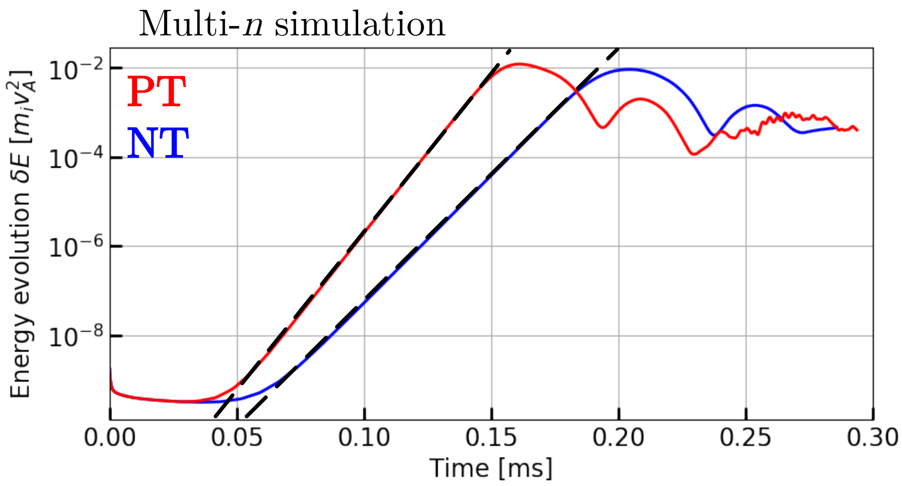

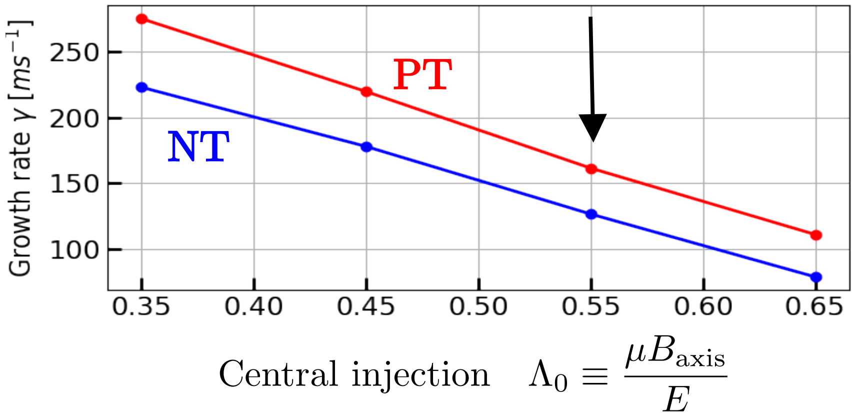

Outline

- Experimental observations of TAEs in NT
- MEGA: 3D nonlinear hybrid kinetic-MHD
- TAEs in NT and PT
- Wave-particle resonances in the FI phase-space
- Fast-ion losses induced by TAE in NT and PT

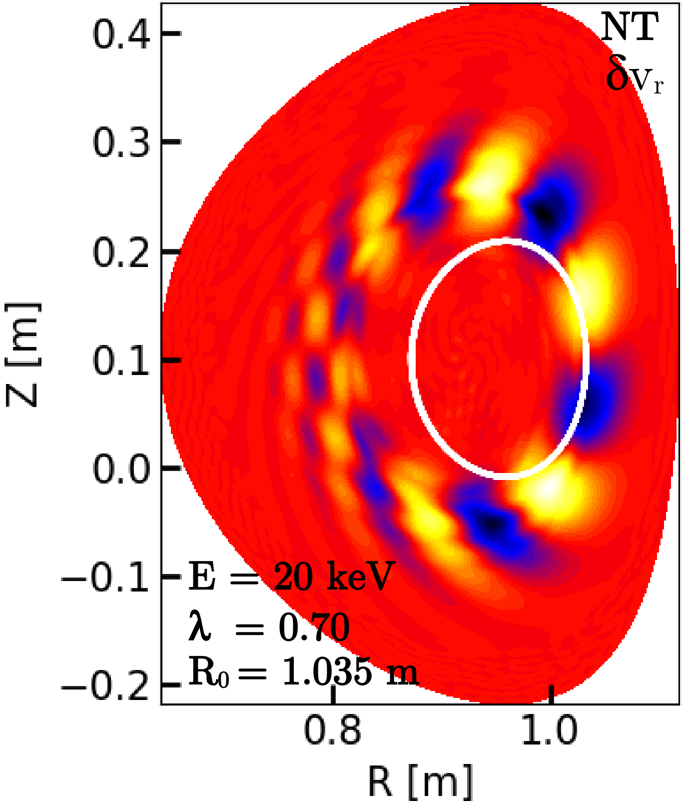

Resonant energy exchange in FI phase-space

- Power exchange in FI phase-space shows particle-wave resonances.

$$\Delta E > 0 \longrightarrow \text{Energy to the FI}$$

$$\Delta E < 0 \longrightarrow \text{Energy to the wave}$$

- Two main regions of the phase-space providing energy to TAE.

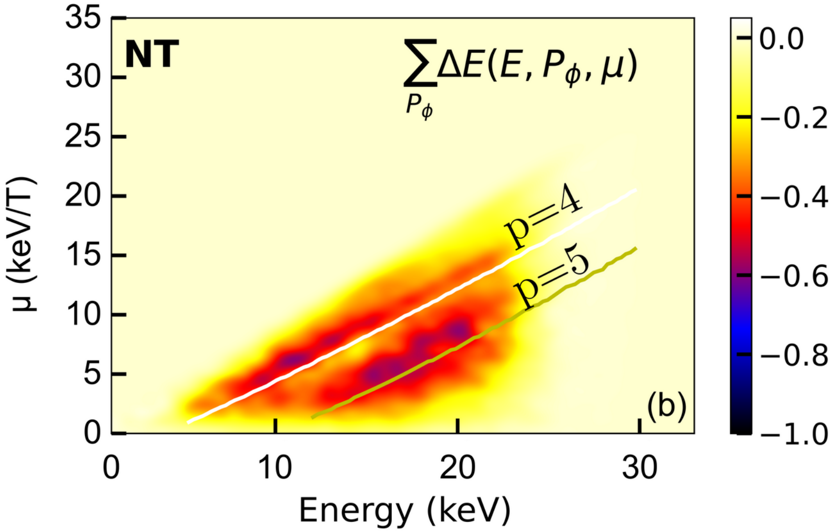

Resonant energy exchange in FI phase-space

- Power exchange in FI phase-space shows particle-wave resonances.

$$\Delta E > 0 \longrightarrow \text{Energy to the FI}$$

$$\Delta E < 0 \longrightarrow \text{Energy to the wave}$$

- Two main regions of the phase-space providing energy to TAE:
  - Wave-particle resonances[9].

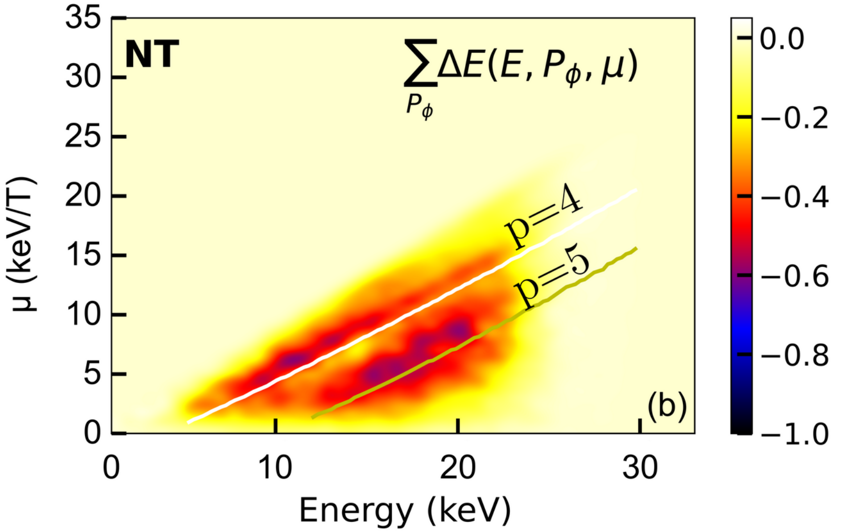

[9] Y. Todo, Rev. Mod. Plasma Phys **3**, 1 (2019)

NT damps the lower bounce harmonic

- Alignment of analytical resonances with structures in FI phase-space.
- In PT, lower transit harmonic is most excited.
- In NT, damps lower transit harmonics.

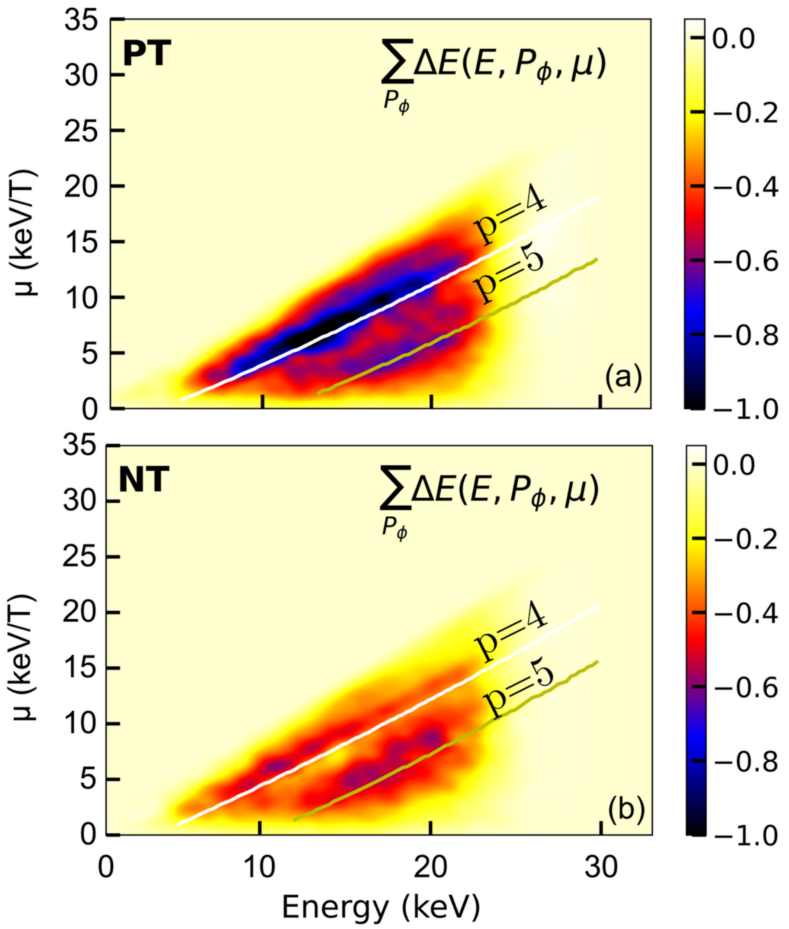

NT damps the lower bounce harmonic.

- Alignment of analytical resonances with structures in FI phase-space.
- In PT, lower transit harmonic is most excited.
- In NT, damps lower transit harmonics.
- Overall energy transfer is larger in PT.

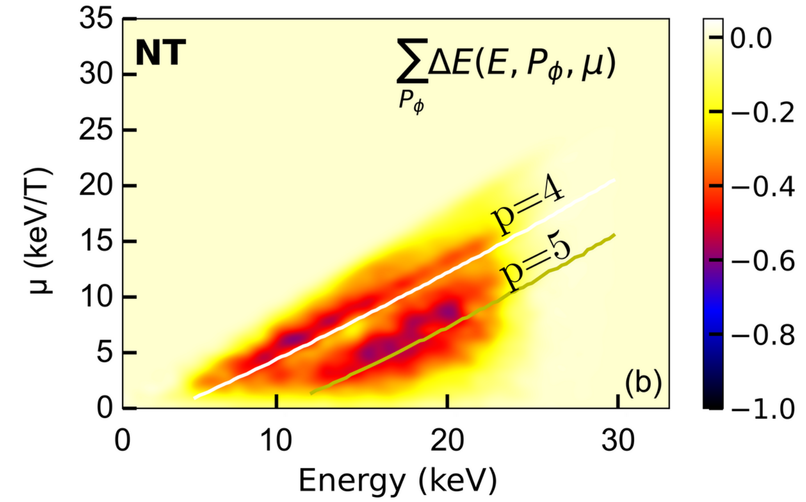

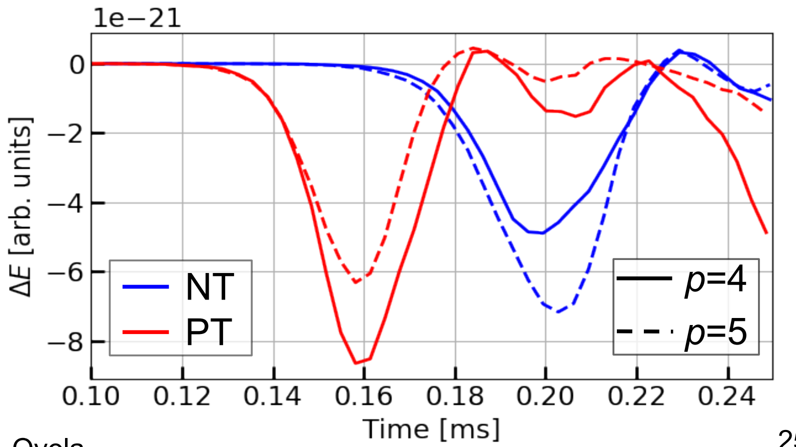

Outline

- Experimental observations of TAEs in NT
- MEGA: 3D nonlinear hybrid kinetic-MHD
- TAEs in NT and PT
- Wave-particle resonances in the FI phase-space
- Fast-ion losses induced by TAE in NT and PT

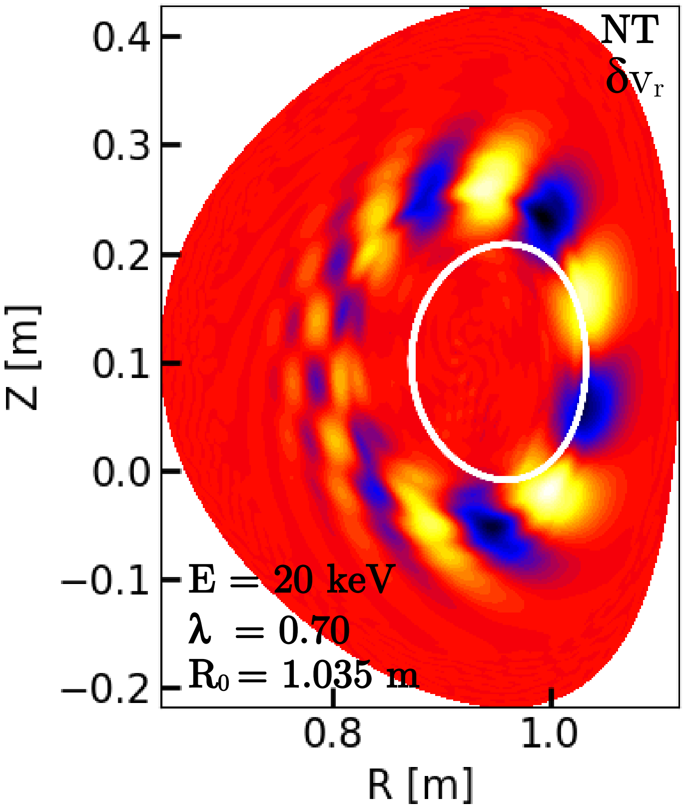

Synthetic wall in MEGA[10]

- 2D wall implemented in MEGA for TCV tokamak.

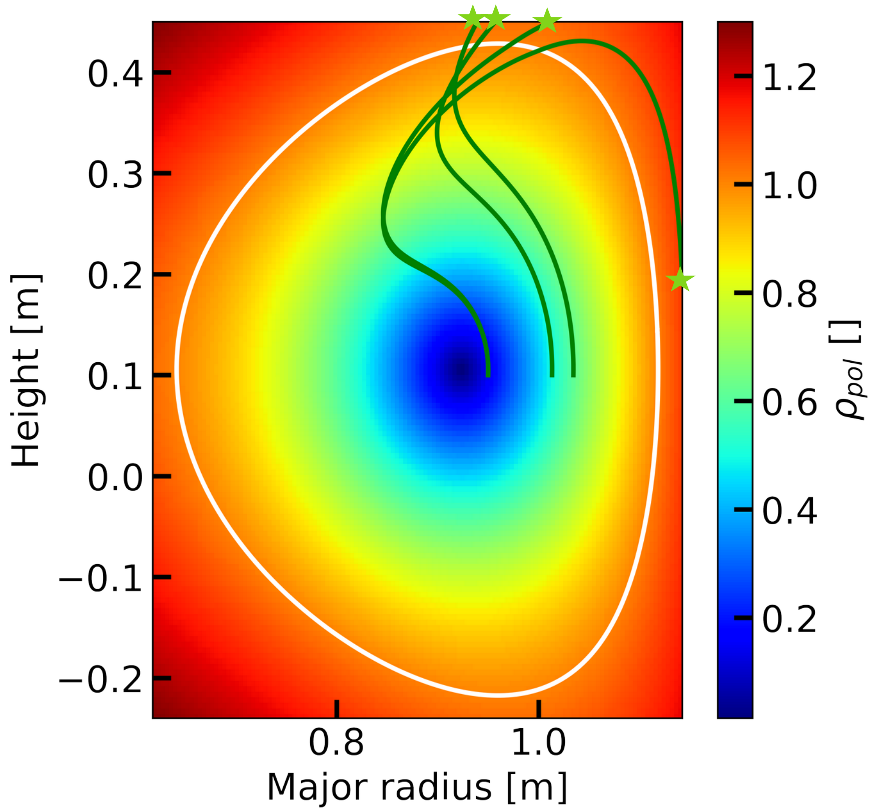

[10] P. Oyola *et al.*, RSI **92** (2021)

TAE-induced FIL are 3x lower in NT

- 2D wall implemented in MEGA for TCV tokamak.
- Correlated FIL bursts with TAE saturation.

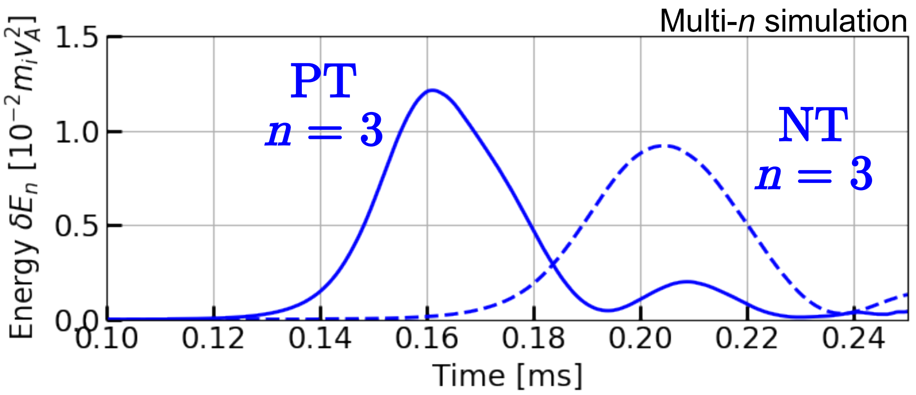

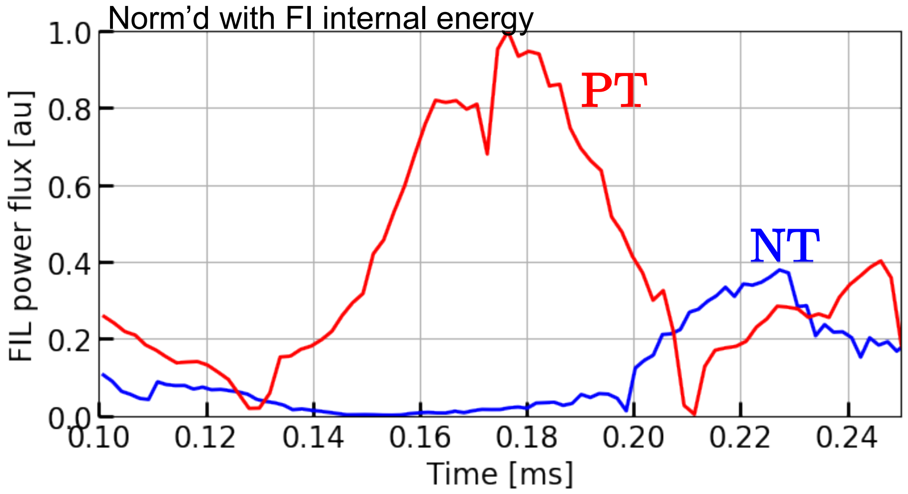

TAE-induced FIL are 3x lower in NT

- 2D wall implemented in MEGA for TCV tokamak.
- Correlated FIL bursts with TAE saturation.
- Fast-ion losses in NT is **smaller** than its counterpart in PT.
  - 3x times lower at the peak.
  - 3x times lower integrated FIL.

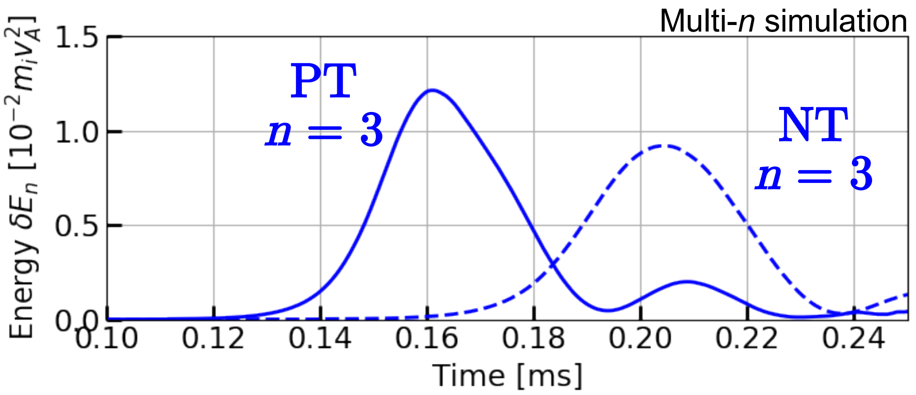

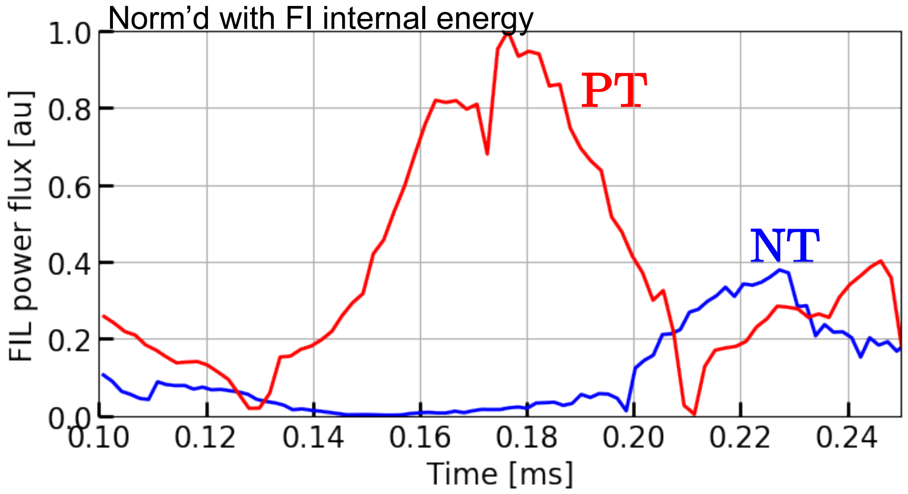

TAE-induced FIL are 3x lower in NT

- 2D wall implemented in MEGA for TCV tokamak.
- Correlated FIL bursts with TAE saturation.
- Fast-ion losses in NT is **smaller** than its counterpart in PT.
  - 3x times lower at the peak.
  - 3x times lower integrated FIL.

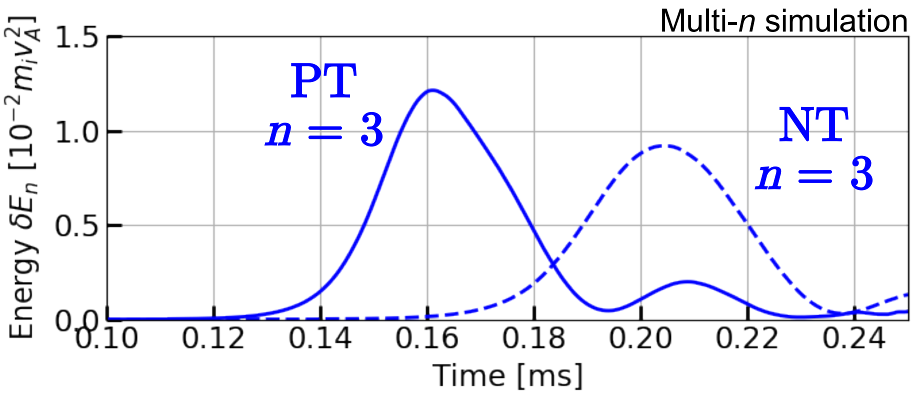

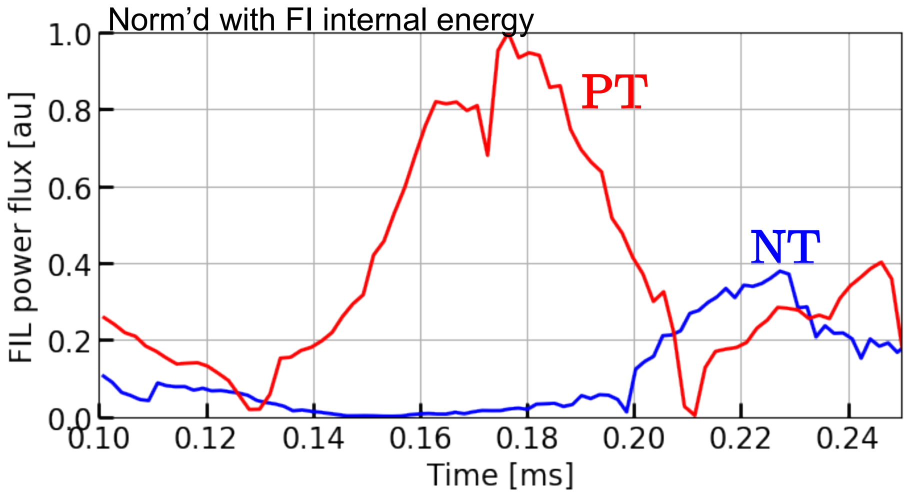

Conclusions & Outlook

- In experiments, TAEs appear weaker in NT than in its counterpart PT.
- MEGA sims used to isolate the δ effects.
- ~40% lower energy in NT with respect to PT.
- Lower transit harmonics are damped in NT.
- Fast-ion losses are 3x lower in NT.

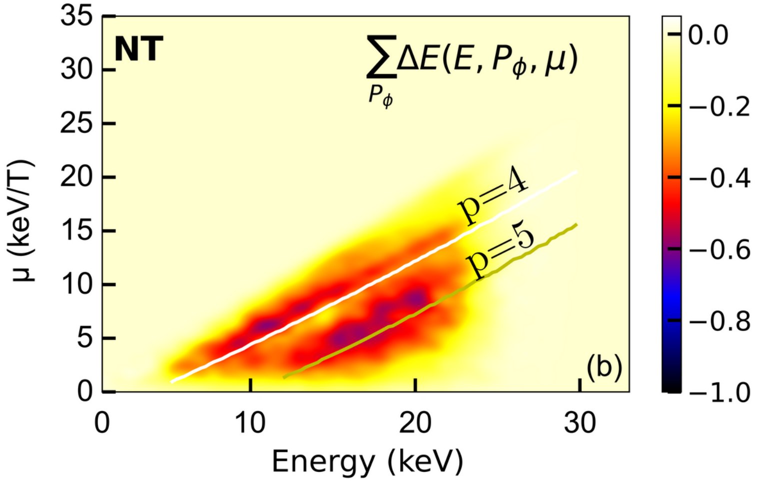

Norm'd with FI internal energy

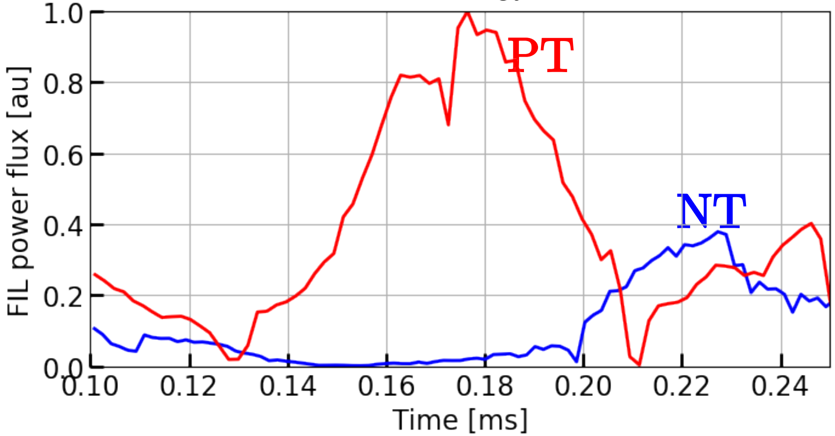

Work-in-progress

- Extend the scan to several δ ∈ (-0.6, 0.6).
- Studying the particle transport by the TAE in both PT and NT.

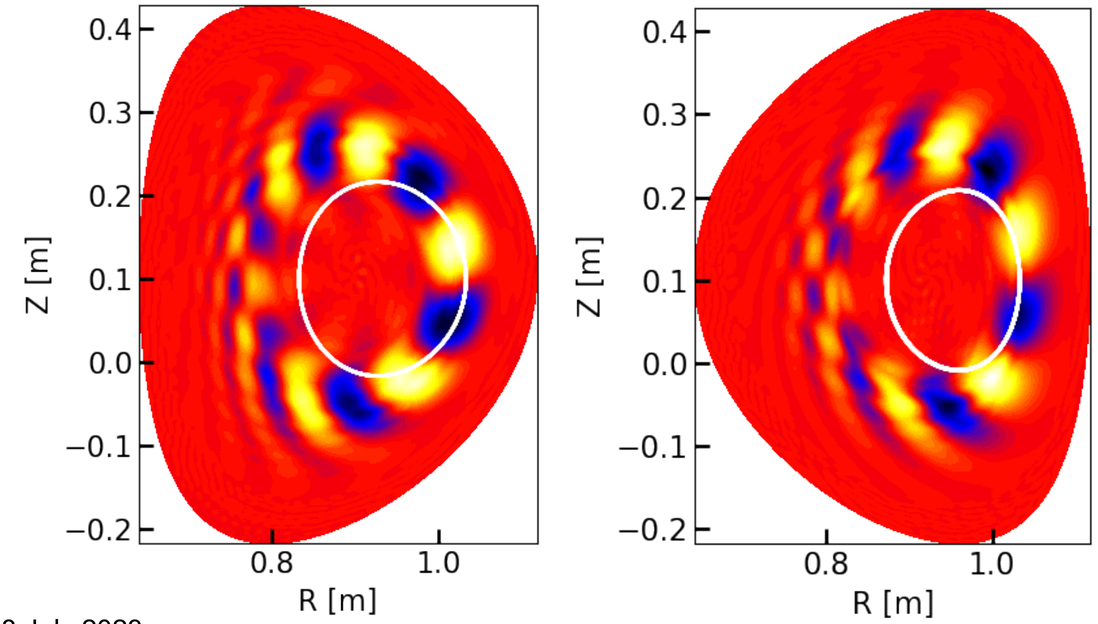

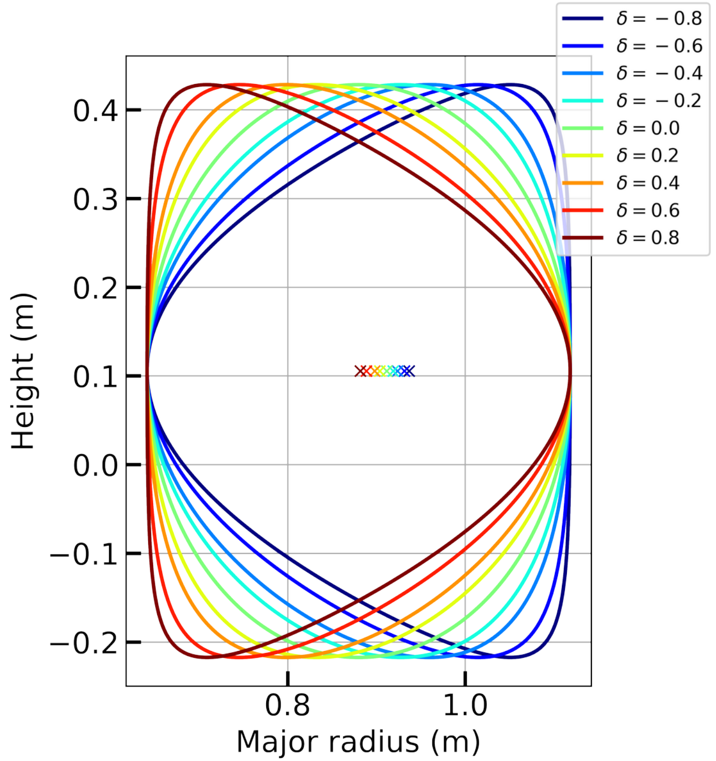

Conclusions & Outlook

- In experiments, TAEs appear weaker in NT than in its counterpart PT.
- MEGA sims used to isolate the δ effects.
- ~40% lower energy in NT with respect to PT.
- Lower transit harmonics are damped in NT.
- Fast-ion losses are 3x lower in NT.

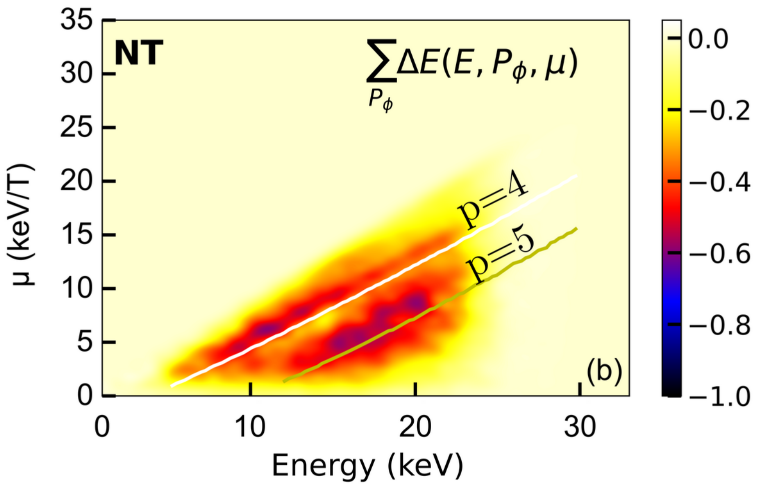

Norm'd with FI internal energy

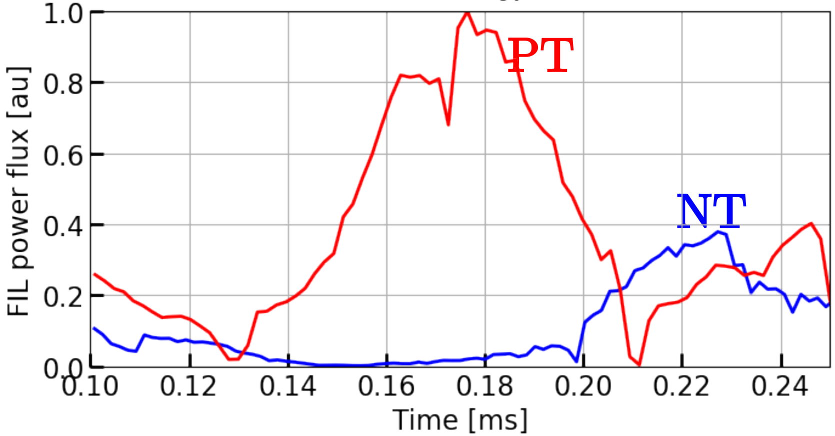

Backup slides

This work has been carried out within the framework of the EUROfusion Consortium and has received funding from the Euratom research and training programme 2014-2018 and 2019-2020 under grant agreement No 633053. The views and opinions expressed herein do not necessarily reflect those of the European Commission.